

# Hydration Layer Coupling and Cooperativity in Phase Behavior of Stimulus Responsive Peptide Polymers

Dennis Kurzbach,<sup>†</sup> Wafa Hassouneh,<sup>‡</sup> Jonathan R. McDaniel,<sup>‡</sup> Eva A. Jaumann,<sup>†</sup> Ashutosh Chilkoti,<sup>‡</sup> Dariush Hinderberger<sup>†\*</sup>

<sup>†</sup> Max Planck Institute for Polymer Research, Ackermannweg 10, 55128 Mainz, Germany

<sup>‡</sup> Department of Biomedical Engineering, Duke University, 136 Hudson Hall, Box 90281, Durham, NC 27708-0281, USA

## - Supporting Information -

### METHODS

Data analysis: All spectral simulations were performed with home-written programs in MATLAB (The MathWorks, Inc.) employing the EasySpin toolbox for EPR spectroscopy.<sup>1</sup> Simulations of CW EPR spectra in fluid solution were performed by using a model, which is based on the slow-motion theory and a program developed by Schneider and Freed as implemented in EasySpin.<sup>2</sup> These simulations can account for the effect of intermediate or slow rotational diffusion of the radical on the EPR spectra. All reported values for hyperfine-coupling parameters were obtained from simulating the experimental CW spectra. The hyperfine-coupling constants are given in MHz throughout this article. 1 MHz corresponds to 0.0357 mT at a magnetic field of 336 mT. Two-component spectra were simulated as weighted sums of double-integral normalized CW EPR spectra,  $S$ , of species A and B:  $S_{exp} = \chi_A S_A + (1 - \chi_A) S_B$ . A partitioning of a probe between regions of different polarity gives rise to a spectral contrast between species A in the polar regions and species B located in the apolar regions. Thus, the mole fraction of species B,  $\chi_B = 1 - \chi_A = n_B / \sum_{i=1} n_i$  is a relative measure of the hydrophobic volume present in a system. Typical g-values for the spectral simulation of component A (hydrophilic) were:  $g_{xx} = 2.0087$ ,  $g_{yy} = 2.0067$ ,  $g_{zz} = 2.0030$ . For species B (hydrophobic):  $g_{xx} = 2.0088$ ,  $g_{yy} = 2.0068$ ,  $g_{zz} = 2.0032$ . The hyperfine tensor,  $\mathbf{A}$ , was simulated with principle values:  $A_{xx} = 18.02$  MHz,  $A_{yy} = 16.84$  MHz and  $A_{zz} = 90.00 - 100.00$  MHz,  $A_{zz}$  depending on the polarity of the probes' environment. Furthermore, an

anisotropic rotational diffusion tensor was assumed with temperature-dependent principal values for species A:  $D_{xx} = 5.0 \cdot 10^9 \text{ s}^{-1}$ ,  $D_{yy} = 5.0 \cdot 10^9 \text{ s}^{-1}$ ,  $D_{zz} = 4.2 \cdot 10^9 - 8.2 \cdot 10^9 \text{ s}^{-1}$ . For species B:  $D_{xx} = 1.0 \cdot 10^8 - 1.2 \cdot 10^8 \text{ s}^{-1}$ ,  $D_{yy} = 1.2 \cdot 10^8 \text{ s}^{-1}$ ,  $D_{zz} = 6.0 \cdot 10^7 - 8.0 \cdot 10^7 \text{ s}^{-1}$ , with Euler angles of the principal diffusion tensor of  $\alpha = 0^\circ$ ,  $\beta = 50^\circ$ ,  $\gamma = 0^\circ$ .  $a_{\text{iso}}$  was calculated as  $\text{tr}(\mathbf{A})/3$ . The rotational correlation time was calculated as:  $\tau_c = 6^{-1}(D_{xx} D_{yy} D_{zz})^{-1/3}$ .

## EXPERIMENTAL

All genes encoding ELPs were synthesized as reported earlier.<sup>3,4</sup> The ELPs were expressed using a previously published hyperexpression protocol, which relies on the leakiness of the T7 promoter.<sup>5</sup> 50 mL cultures grown for 16 h were used to inoculate six 1 L flasks of TBDry supplemented with 100  $\mu\text{g/mL}$  ampicillin (ELP1) or 45  $\mu\text{g/mL}$  kanamycin (ELP2). Each 1 L flask was then incubated at 37 °C for 24 hrs and 210 rpm, after which the cell suspension was centrifuged at 3,000 rpm for 10 min at 4 °C. Each ELP was purified using Inverse Transition Cycling, which has been described elsewhere.<sup>6</sup> Briefly, the cell pellet was resuspended in PBS and lysed via sonication on ice for 3 mins (10 s on, 40 s off) (Masonix S-4000; Farmingdale, NY). Polyethyleneimine (PEI) 0.7% w/v was added to the lysate to precipitate nucleic acid contaminants. The supernatant was then subjected to multiple rounds of ITC as follows. The solution was heated to 37 °C in the presence of 3 M NaCl. The coacervate was centrifuged for 10 min at 14,000 g and 20 °C, and resuspended in 20 mM TCEP in water, pH 7. This suspension was cooled to 4 °C, and then centrifuged for 10 min at 14,000 and 4 °C to remove any insoluble contaminants. Typically, 3-5 rounds of ITC generated a sufficiently pure product (>95% by SDS-PAGE).

The amino acid sequences of all used ELPs were: For  $V_1H_2G_1A_1-120$  MSKGGP(VPGVG-VPGHG-VPGGG-VPGHG-VPGAG)<sub>24</sub>WP; for  $V_1H_4-80$  MSKGGP(VPGVG-(VPGHG)<sub>4</sub>)<sub>20</sub>WP; for  $V_1G_7A_8-96$  MSKGGP(VPGVG-(VPGAG-VPGGG)<sub>7</sub>-VPGAG)<sub>6</sub>WP; for  $V_1G_7A_8-160$  MSKGGP(VPGVG-(VPGAG-VPGGG)<sub>7</sub>-VPGAG)<sub>10</sub>WP; for  $K_1V_6-56$

MSKGPG(VPGKG-(VPGVG)<sub>6</sub>)<sub>8</sub>WP; for K<sub>1</sub>V<sub>16</sub>-204 MSKGPG(VPGKG-(VPGVG)<sub>16</sub>)<sub>12</sub>WP; for A-y SKGPG(VPGAG)<sub>y</sub>Y; for A<sub>8</sub>V<sub>2-y</sub> SKGPG (VPGVG-(VPGAG)<sub>4</sub>)<sub>y/5</sub>WP; for A<sub>5</sub>V<sub>5-y</sub> SKGPG (VPGVG-VPGAG)<sub>y/2</sub>WP; for A<sub>2</sub>V<sub>8-y</sub> SKGPG ((VPGVG)<sub>4</sub>-VPGAG)<sub>y/5</sub>Y; for V-y SKGPG (VPGVG)<sub>y</sub>Y.

Sample Preparation: 1 wt % of an ELP was dissolved in PBS, containing 3 mM KCl and 140 mM NaCl at the desired pH. Afterwards 1 v/v % of a 100 mM 16-DSA (16-DOXYL stearic acid) ethanol solution was added to the sample to yield a final spin-probe concentration of 1 mM. The samples were subsequently transferred into 3 mm outer diameter quartz tubes for continuous wave (CW) EPR.

EPR Measurements: Field-swept CW EPR spectra at X-band (~9.4 GHz) were measured on a Magnettech (Berlin, Germany) MiniScope MS200 benchtop CW EPR spectrometer with a variable-temperature cooling/heating unit (TC HO2). The temperature was varied in steps of 2°C. After every temperature change the sample was left to equilibrate for 10 min. No changes in the spectra were observed for longer waiting periods. The sample volume was always large enough to fill the complete resonator volume in the probehead (>300 µL).

#### RATIONALE OF THE SPIN PROBING APPROACH

If for a spin probe (here 16-DSA) hydrophobic regions in an otherwise aqueous environment are available, the probe is partitioned between the aqueous and the hydrophobic environments. Since the electron spin population (density) at the nitrogen nucleus of the DOXYL group of 16-DSA depends on the polarity of the molecule's direct environment, the hyperfine interaction or, more precisely, the coupling between the electron spin and the nuclear spin of <sup>14</sup>N of the nitroxide moiety (see Figure 1) is sensitive to environmental polarity, too. Such, a partitioning of 16-DSA between regions of different hydrophobicity gives rise to a spectral contrast between a spectral 16-DSA species *A* in the hydrophilic regions and a species *B* located in the hydrophobic regions. Thus, the mole fraction of species

B,  $\chi_B = n_B / \sum_{i=1} n_i$  is a relative measure of the hydrophobic volume present in a system. Further, the isotropic hyperfine coupling constant,  $a_{iso}$ , of species B is a measure for the hydrophobicity of the hydrophobic environment.<sup>7</sup> Such, by adding 16-DSA to an aqueous solution of a thermoresponsive polymer and by following the temperature dependence of its CW EPR spectrum, one can detect the occurrence and polarity of hydrophobic cavities of any kind. These cavities form during the temperature-induced collapse of polymer strands and the amphiphilic spin probe is incorporated to some extent. This happens regardless of the precise collapse mechanism, whether e.g. one has a unimer collapse<sup>8</sup>, micellization<sup>9</sup>, 3D-network collapse<sup>10</sup> etc. It should be noted that the hyperfine tensor,  $\mathbf{A}_i$ , of the effective spin-Hamiltonian

$$H = H_{Electron-Zeeman} + H_{Hyperfine} = \frac{\beta_e}{\hbar} \mathbf{B}^T \mathbf{g} \mathbf{S} + \sum_{i=1}^N \mathbf{S}^T \mathbf{A}_i \mathbf{I}_i$$

is completely independent of the g-tensor,  $\mathbf{g}$ , which describes the field position of the spectrum at a given frequency.  $\mathbf{g}$  typically shifts to lower field-positions with increasing hydrophobicity of a spin's environment.<sup>11</sup> Hence, as depicted in Figure 1, the most prominent effects can be observed at the high-field line of a nitroxide spectrum, where A- (larger) and g- (to lower fields) shifts add up. We hence focus on this line throughout this article.

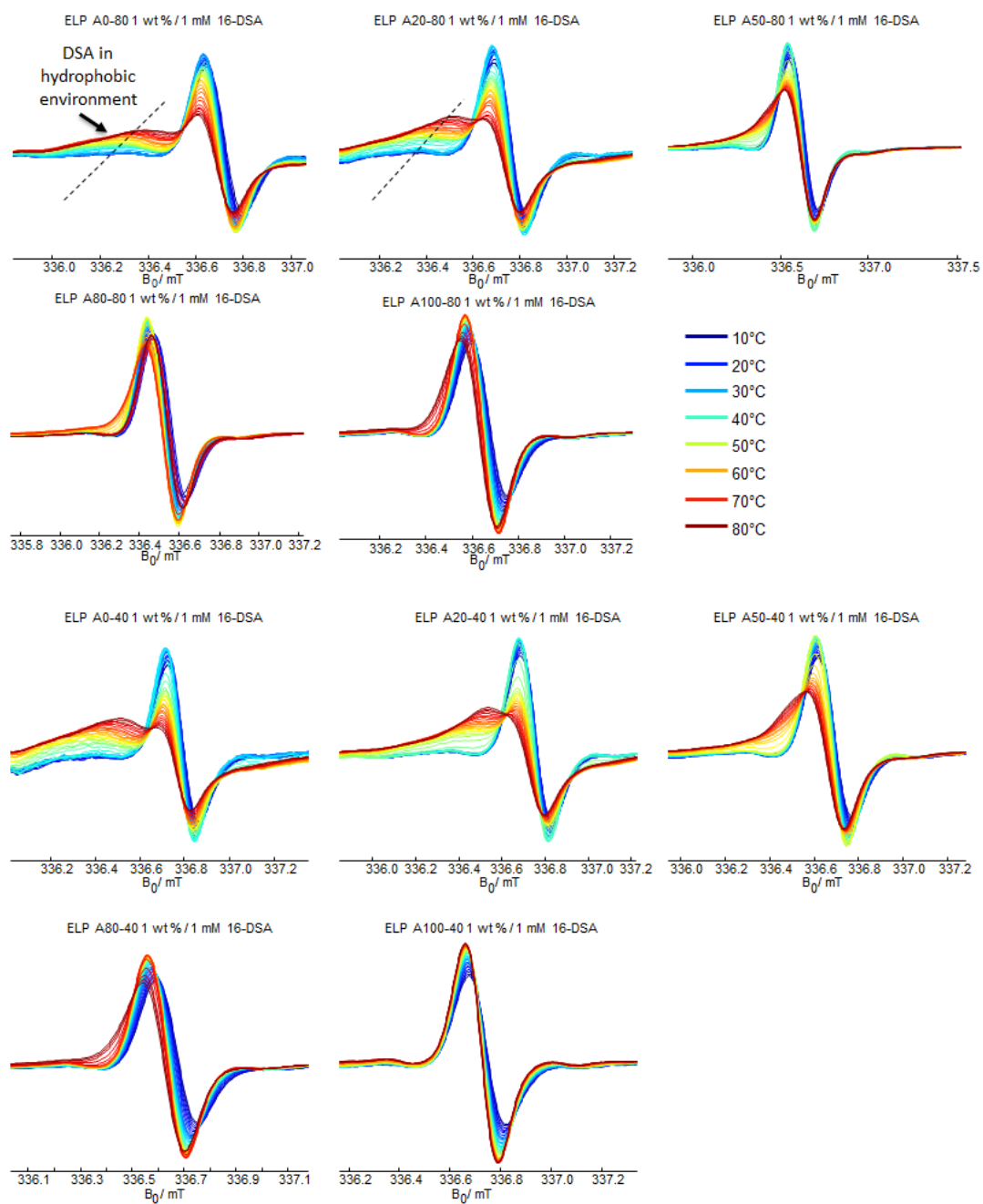


**Figure S1.** High-field transitions of experimental CW EPR spectra of 1 mM 16-DSA for solutions of all ELPs under investigation. The temperature range is 10°C to 80°C in steps of 2°C. The color code is shown in the figure.

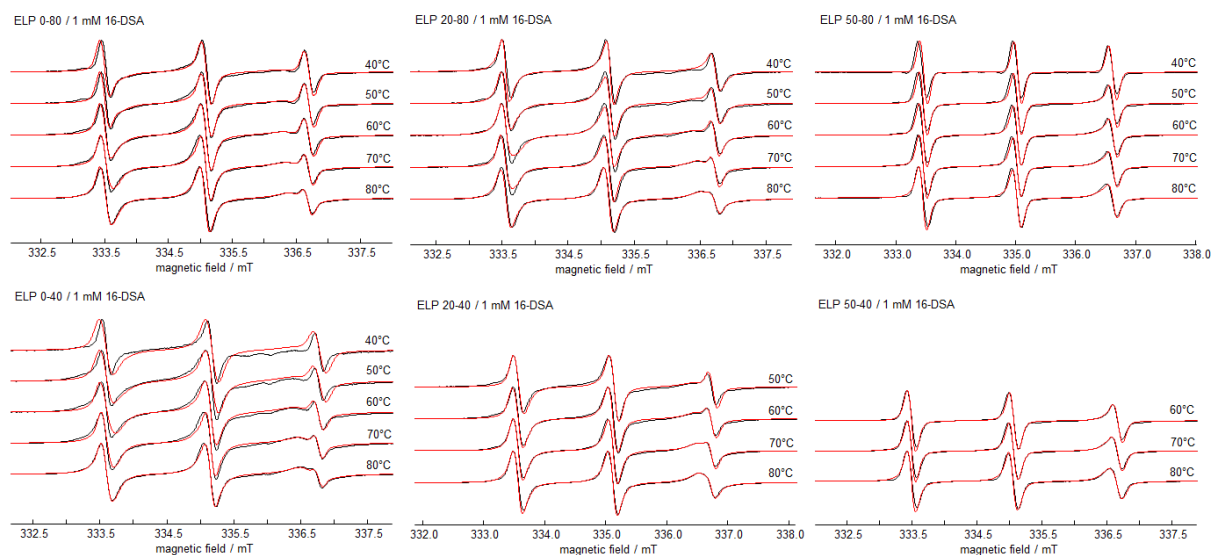


**Figure S2.** Experimental spectra (black) and corresponding simulations (red) for selected detected two-component spectra of 1 mM 16-DSA in 1 wt% ELP solutions in temperature intervals of 10°C.

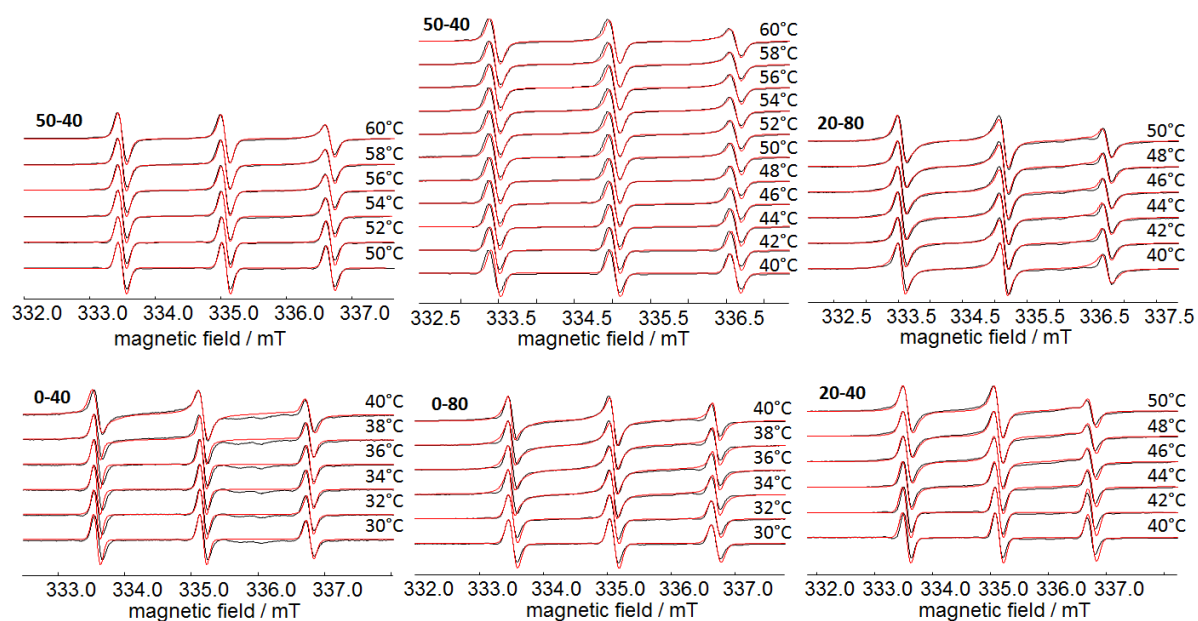


**Figure S3.** Experimental spectra (black) and corresponding simulations (red) for selected detected two-component spectra of 1 mM 16-DSA in 1 wt% ELP solutions in temperature intervals of 2°C.

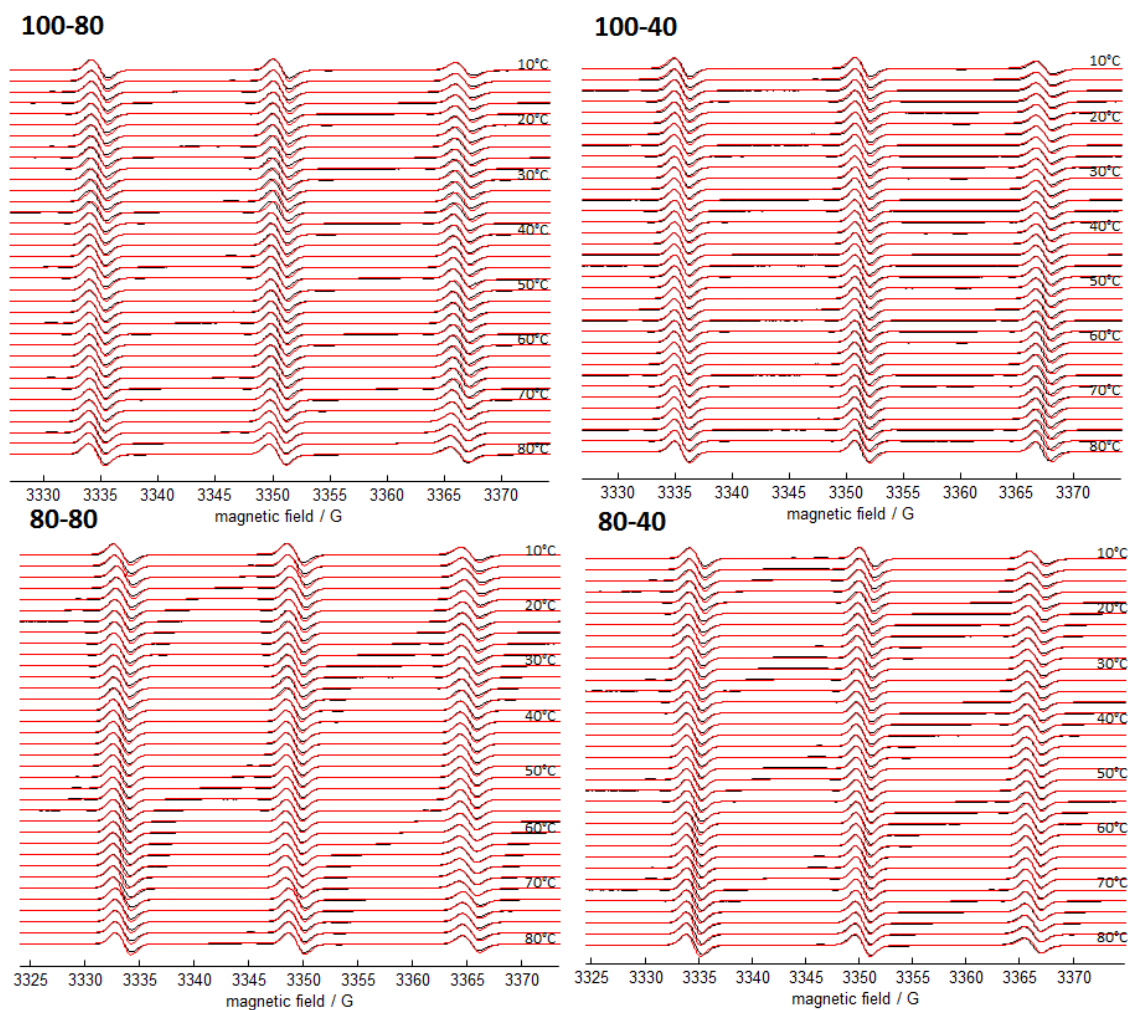


**Figure S4.** Experimental spectra (black) and corresponding simulations (red) for one-component spectra of 1 mM 16-DSA in 1 wt% ELP solutions in temperature intervals of 2°C

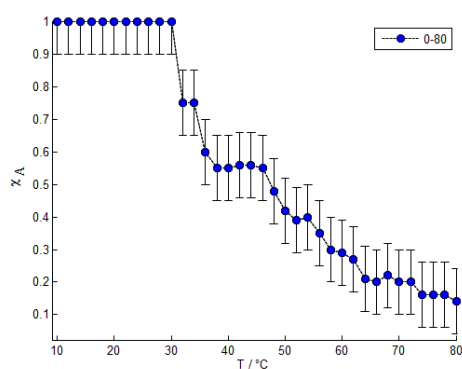


**Figure S5.**  $\chi_A$  for ELP 0-80 at 10 wt %. As can be observed the transition is still broad, like in the case of 1 wt %. Hence, the sharp phase transition of x-40 ELPs is not a consequence of higher molar concentrations at 1 wt % due to lower molecular weight, compared to the x-80 ELPs.

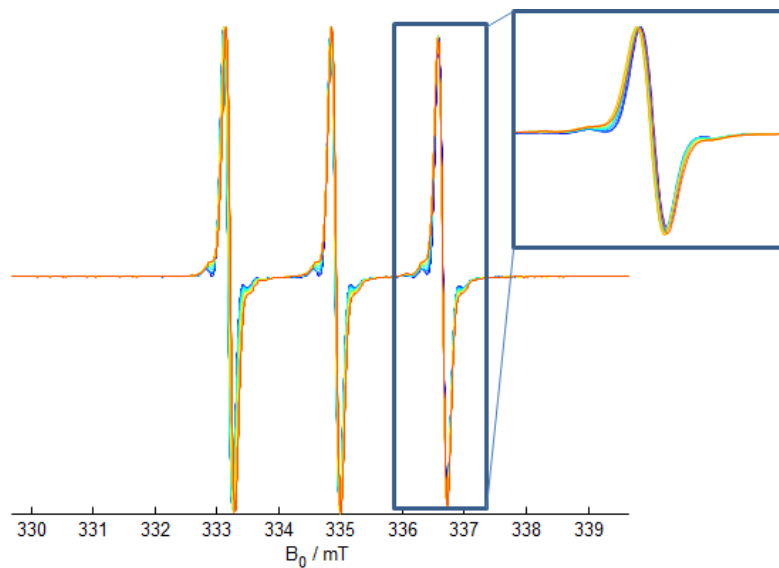


**Figure S6.** CW EPR of 1 wt % ELP 0-80 with 0.2 mM TEMPO. No significant interaction with the ELP aggregates (incorporation) can be observed.

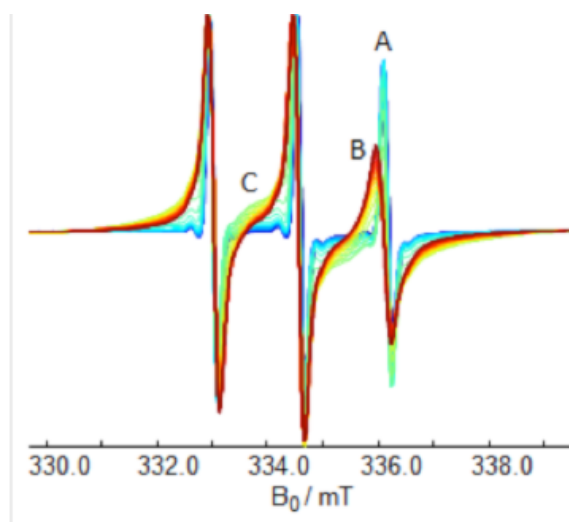


**Figure S7.** CW EPR of 1 wt % ELP K<sub>1</sub>V<sub>6</sub>-56 with 1 mM 16-DSA at pH 10. Species C is still visible.



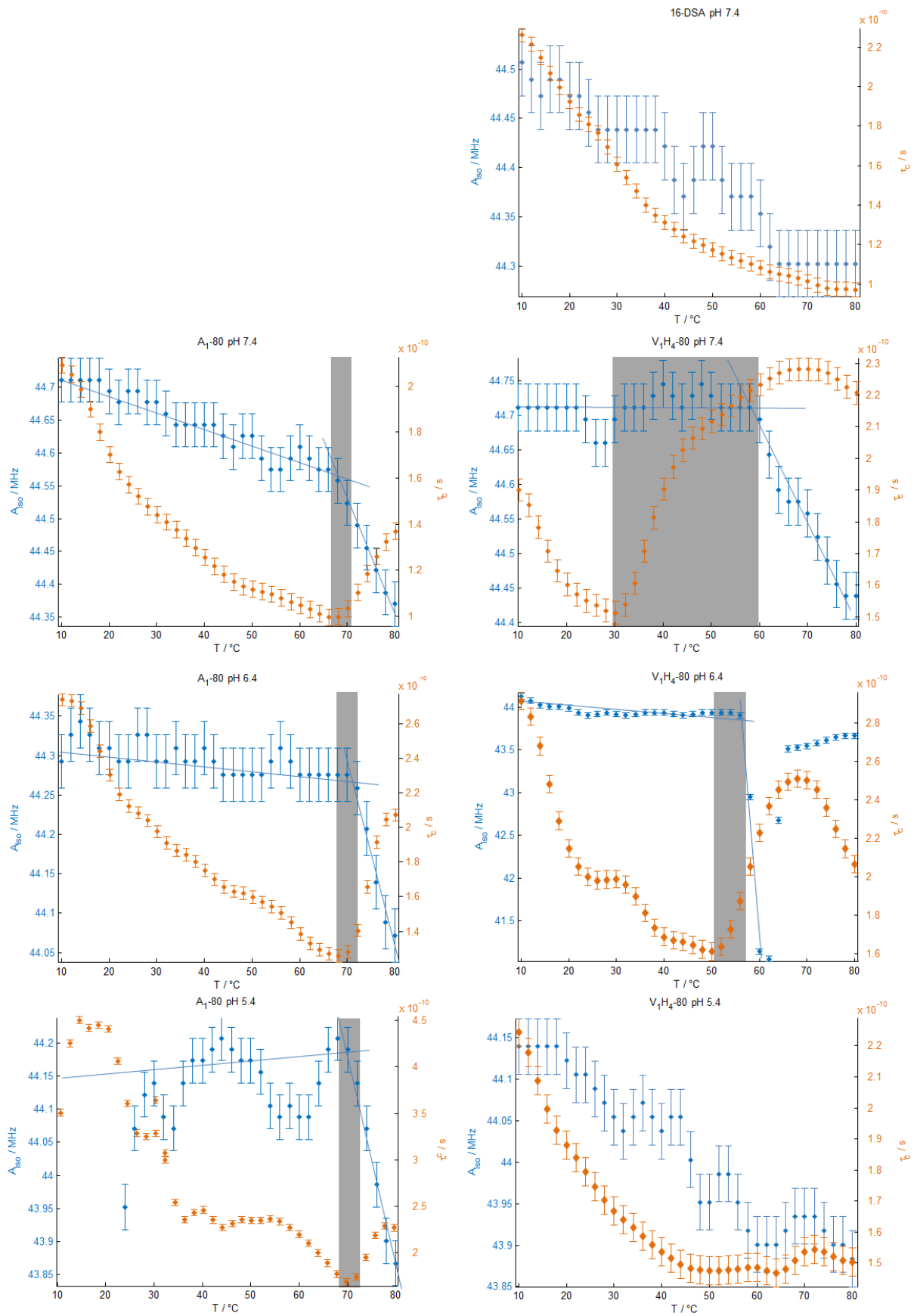


**Figure S8.** Rotational correlation times,  $\tau_c$ , and isotropic hyperfine splitting ( $a_{\text{iso}}$ ) of selected ELPs (see headings in the figure). The grey bars indicate the difference between phase transitions observed through  $\tau_c$  and  $a_{\text{iso}}$ .

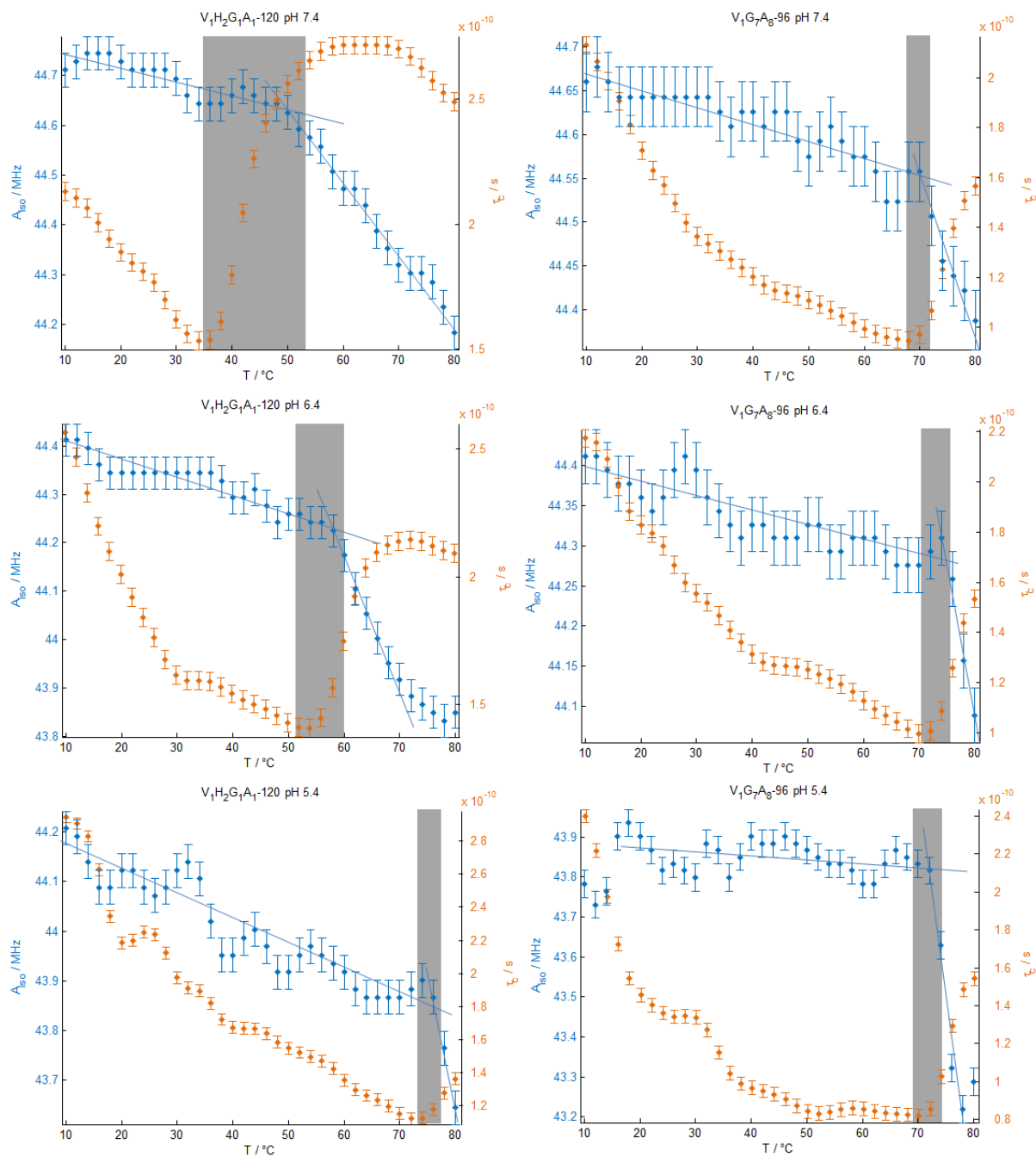


**Figure S8.** Continued.

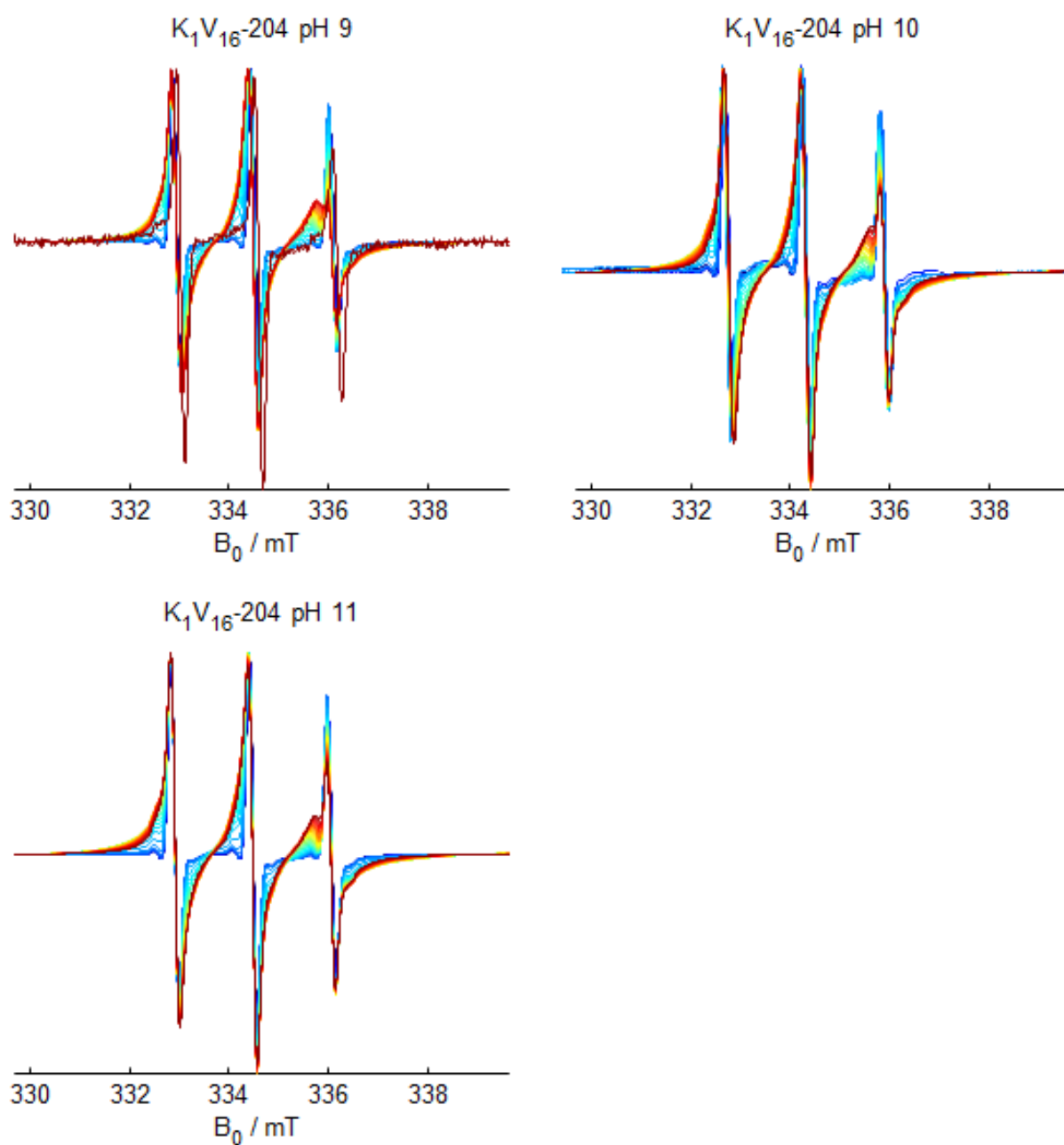


**Figure S9.** CW EPR of 1 wt % ELP K<sub>1</sub>V<sub>16</sub>-204 with 1 mM 16-DSA at different pH.

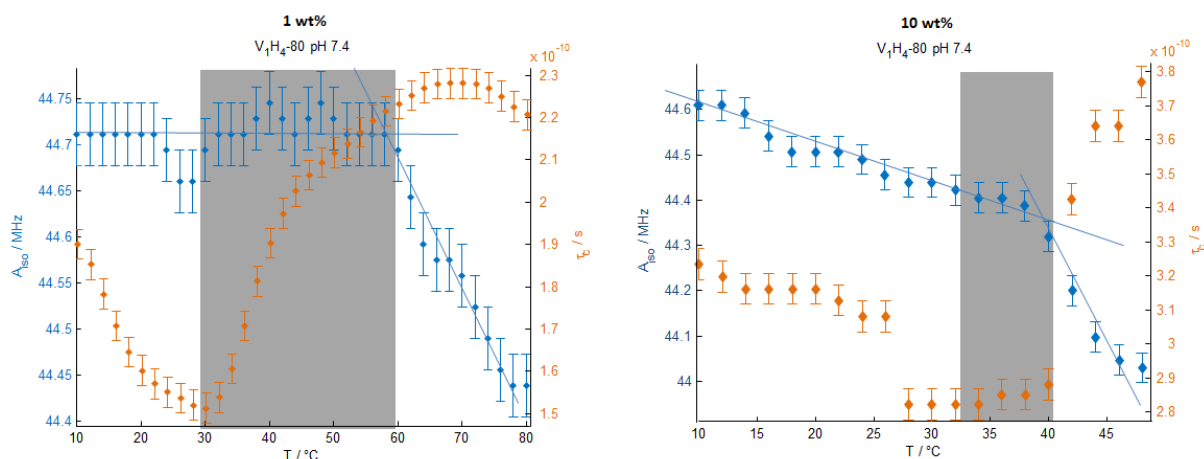


**Figure S10.** Rotational correlation times,  $\tau_c$ , and isotropic hyperfine splitting ( $a_{\text{iso}}$ ) of ELP  $V_1H_4$ -80 at pH 7.4 at different concentrations (1 wt% and 10 wt%; see headings in the figure). The grey bars indicate the difference between phase transitions observed through  $\tau_c$  and  $a_{\text{iso}}$ .

## REFERENCES

- (1) Stoll, S.; Schweiger, A. *J. Magn. Reson.* **2006**, *178*, 42.
- (2) Schneider, D. J.; Freed, J. H. *Biological Magnetic Resonance Vol 8. Theory and Applications*; Plenum Press: New York, 1889.
- (3) McDaniel, J. R.; MacKay, J. A.; Quiroz, F. G.; Chilkoti, A. *Biomacromolecules* **2010**, *11*, 944.
- (4) MacKay, J. A.; Callahan, D. J.; FitzGerald, K. N.; Chilkoti, A. *Biomacromolecules* **2010**, *11*, 2873.
- (5) Zhang, X.; Guda, C.; Datta, R.; Dute, R.; Urry, D. W.; Daniell, H. *Biotechnology Letters* **1995**, *17*, 1279.
- (6) Meyer, D. E.; Chilkoti, A. *Nature Biotechnology* **1999**, *17*, 1112.
- (7) Knauer, B. R.; Napier, J. J. *J. Am. Chem. Soc.* **1976**, *98*, 4395.
- (8) Wu, C.; Zhou, S. *Macromolecules* **1995**, *28*, 5388.
- (9) Alexandridis, P.; Hatton, T. A. *Colloids and Surfaces A* **1995**, *96*, 1.
- (10) Junk, M. J. N.; Jonas, U.; Hinderberger, D. *Small* **2008**, *4*, 1485.
- (11) Weil, J. A.; Bolton, J. R.; Weitz, J. E. *Electron paramagnetic resonance: Elementary theory and applications*; Wiley-interscience: New York, 2007; Vol. 2.